

# Accelerated Degradation Tests: Modeling and Analysis

William Q. Meeker  
Dept. of Statistics and  
Center for Nondestructive Evaluation  
Iowa State University  
Ames, IA 50011

Luis A. Escobar  
Dept. of Experimental Statistics  
Louisiana State University  
Baton Rouge, LA 70803

C. Joseph Lu  
Department of Statistics  
National Cheng-Kung University  
Tainan, Taiwan

September 20, 1999

## Abstract

High reliability systems generally require individual system components having extremely high reliability over long periods of time. Short product development times require reliability tests to be conducted with severe time constraints. Frequently few or no failures occur during such tests, even with acceleration. Thus, it is difficult to assess reliability with traditional life tests that record only failure times. For some components, degradation measures can be taken over time. A relationship between component failure and amount of degradation makes it possible to use degradation models and data to make inferences and predictions about a failure-time distribution.

This paper describes degradation reliability models that correspond to physical-failure mechanisms. We explain the connection between degradation reliability models and failure-time reliability models. Acceleration is modeled by having an acceleration model that describes the effect that temperature (or another accelerating variable) has on the rate of a failure-causing chemical reaction. Approximate maximum likelihood estimation is used to estimate model parameters from the underlying mixed-effects nonlinear regression model. Simulation-based methods are used to compute confidence intervals for quantities of interest (e.g., failure probabilities). Finally we use a numerical example to compare the results of accelerated degradation analysis and traditional accelerated life test failure-time analysis.

**Key words:** Bootstrap, Maximum likelihood, Mixed effects, Nonlinear estimation, Random effects, Reliability.

# 1 Introduction

## 1.1 Background

Today's manufacturers face strong pressure to develop newer, higher technology products in record time, while improving productivity, product field reliability, and overall quality. This has motivated the development of methods like concurrent engineering and encouraged wider use of designed experiments for product and process improvement efforts. The requirements for higher reliability have increased the need for more *up-front* testing of materials, components and systems. This is in line with the generally accepted modern quality philosophy for producing high reliability products: achieve high reliability by improving the design and manufacturing processes, moving away from reliance on inspection to achieve high reliability.

Estimating the failure-time distribution or long-term performance of components of *high reliability* products is particularly difficult. Many modern products are designed to operate without failure for years, tens of years, or more. Thus few units will fail or degrade importantly in a test of practical length at normal use conditions. For example, during the design and construction of a communications satellite, there may be only 6 months available to test components that are expected to be in service for 15 or 20 years. For this reason, Accelerated Tests (ATs) are used widely in manufacturing industries, particularly to obtain timely information on the reliability of product components and materials. Generally, information from tests at high levels of accelerating variables (e.g., use rate, temperature, voltage, or pressure) is extrapolated, through a physically reasonable statistical model, to obtain estimates of life or long-term performance at lower, normal use conditions. In some cases the level of an accelerating variable is increased or otherwise changed during the course of a test (step-stress and progressive-stress ATs). AT results are used in design-for-reliability processes to assess or demonstrate component and subsystem reliability, certify components, detect failure modes, compare different manufacturers, and so forth. ATs have become increasingly important because of rapidly changing technologies, more complicated products with more components, and higher customer expectations for better reliability.

## 1.2 Accelerated degradation data

In some reliability studies, it is possible to measure degradation directly over time, either continuously or at specific points in time. In most reliability testing applications, degradation data, if available, can have important practical advantages:

- Degradation data can, particularly in applications where few or no failures are expected, provide considerably more reliability information than would be available from traditional censored failure-time data.
- Accelerated tests are commonly used to obtain reliability test information more quickly. Direct observation of the *degradation process* (e.g., tire wear) may allow direct modeling of the failure-causing mechanism, providing more credible and precise reliability estimates and a firmer basis for often-needed extrapolation. Modeling degradation of *performance output* of a component or subsystem (e.g., voltage or power) may be

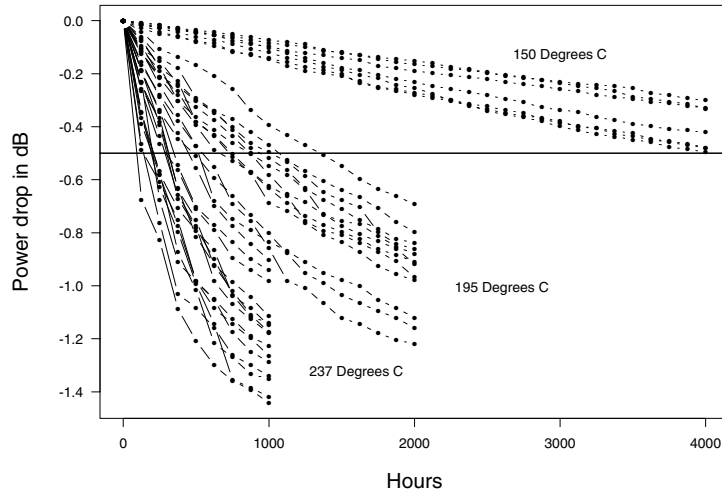


Figure 1: Accelerated degradation test results giving power drop in Device-B output for a sample of units tested a three levels of temperature.

useful, but modeling could be more complicated or difficult because the output may be affected, unknowingly, by more than one physical/chemical failure-causing process.

**Example 1 Device-B power output degradation.** Figure 1 shows the decrease in power, over time, for a sample of integrated circuit devices called “Device-B.” Samples of devices were tested at each of three levels of temperature. At standard operating temperatures (e.g., 80°C junction temperature), the devices will degrade slowly. Based on a life test of about 6 months, design engineers needed an assessment of the proportion of these devices that would “fail” before 15 years (about 130,000 hours) of operation at 80°C junction temperature. This assessment would be used to determine the amount of redundancy required in the full system. Failure for an individual device was defined as power output more than .5 decibels (dB) below initial output. Because they degrade more slowly, units at low temperature had to be run for longer periods of time to accumulate appreciable degradation. Because of severe limitations in the number of test positions, fewer units were run at lower temperatures. The original data from this experiment are proprietary. The data shown in Figure 1 were actually simulated from a model suggested by limited real data available at the time the more complete experiment was being planned. ■

### 1.3 Literature

Shiomi and Yanagisawa (1979) and Suzuki, Maki, and Yokogawa, (1993) describe the analysis of accelerated degradation data on carbon-film resistors. Carey and Tortorella (1988) describe a 3-stage method of estimating parameters of an accelerated degradation model for MOS devices. Chapter 11 of Nelson (1990) describes applications and models for accelerated degradation and describes Arrhenius analysis for data involving a destructive test

(only one degradation reading on each unit). Carey and Koenig (1991) describe an application of the Carey and Tortorella (1988) methods of accelerated degradation analysis in the assessment of the reliability of a logic device. Tobias and Trindade (1995) illustrate the use of some simple linear regression methods for analyzing degradation data. Murray (1993, 1994) and Murray and Maekawa (1996) use such methods to analyze accelerated degradation test data for data-storage disk error rates. Tseng, Hamada, and Chiao (1995) use similar methods with experimental data on lumens output from fluorescent light bulbs over time. Boulanger and Escobar (1994) describe methods for planning accelerated degradation tests for an important class of degradation models. Tseng and Yu (1997) propose methods for choosing the time to terminate a degradation test. Lu and Meeker (1993) fit a random effects model to fatigue degradation data and then use simulation-based methods to make inferences about the corresponding failure-time distribution. In this paper we extend the approach of Lu and Meeker (1993) to allow for acceleration.

## 1.4 Overview

This paper is organized as follows. Section 2 describes useful models for degradation processes at a particular level of an accelerating variable while Section 3 presents models that can be used to relate degradation level and failure time. Section 4 describes methods and models relating degradation to acceleration variables like increased temperature. Section 5 shows how to compute approximate ML estimates of accelerated degradation model parameters. Section 6 shows how to evaluate a failure time cdf for a specified degradation model and use the results from degradation analysis to estimate a failure-time distribution. Section 7 describes and illustrates the use of a parametric bootstrap algorithm to compute confidence intervals for quantities of interest. Section 8 compares the results obtained using accelerated degradation analysis with those from a traditional accelerated life test analyses. In Section 9 we conclude with discussion of some areas for further research.

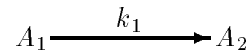
# 2 Models for Degradation

## 2.1 Degradation leading to failure

Many product failures can be traced to an underlying degradation process. The horizontal line in Figure 1 at degradation level  $-0.5$  dB represents the level (or approximate level) at which failure would occur. The failure level (e.g., the horizontal line in Figure 1 at  $-0.5$  dB) may be fixed or random from unit-to-unit. In some applications there will be more than one degradation variable (or more than one underlying degradation process). Here we consider only a single degradation variable.

**Example 2 Degradation from a first-order chemical reaction.** Meeker and LuValle (1995) describe models for growth of failure-causing conducting filaments of chlorine-copper compounds in printed-circuit boards. In their models,  $A_1(t)$  is the amount of chlorine available for reaction and  $A_2(t)$  is proportional to the amount of failure-causing chlorine-copper compounds at time  $t$ . Under appropriate conditions of temperature, humidity, and electrical charge, there will be a chemical reaction in which copper combines with chlorine ( $A_1$ ) to produce  $A_2$ . In the simplest model suggested by Meeker and LuValle (1995), this reaction

occurs in a single step with rate constant  $k_1$ . Diagrammatically,



and the rate equations for this reaction are

$$\frac{dA_1}{dt} = -k_1 A_1 \quad \text{and} \quad \frac{dA_2}{dt} = k_1 A_1, \quad k_1 > 0. \quad (1)$$

The solution of this system of differential equations gives

$$\begin{aligned} A_1(t) &= A_1(0) \exp(-k_1 t) \\ A_2(t) &= A_2(0) + A_1(0)[1 - \exp(-k_1 t)] \end{aligned}$$

where  $A_1(0)$  and  $A_2(0)$  are initial conditions. If  $A_2(0) = 0$ , letting  $A_2(\infty) = \lim_{t \rightarrow \infty} A_2(t) = A_1(0)$ , gives

$$A_2(t) = A_2(\infty)[1 - \exp(-k_1 t)]. \quad (2)$$

The asymptote at  $A_2(\infty)$  reflects the limited amount of chlorine available for reaction to the harmful compounds. ■

Carey and Tortorella (1988) and Carey and Koenig (1991) use similar models to describe degradation of electronic components. As explained in Example 3, here we will use the same first-order chemical reaction model to describe power drop as a function of time, where power drop at time  $t$  will be assumed to be proportional to  $A_2(t)$ . Meeker and LuValle (1995) suggest other more elaborate, but plausible, models for their particular failure mechanism. Section 4 describes the ideas behind acceleration of failure-causing processes.

## 2.2 Variation in degradation and failure time

Variability causes manufactured units to fail at different times. A degradation model should account for the important sources of variability in a failure process. Figure 2 shows degradation curves with unit-to-unit variability in both  $A_2(\infty)$  and  $k_1$ . Having variability in both parameters causes crossing of the curves, typical of what is observed in actual degradation testing. These curves describe unit-to-unit variability in materials properties and initial conditions.

In other applications, individual units will vary with respect to the amount of material available to wear, initial level of degradation, amount of harmful degradation-causing material, and so on. For some applications the variable of interest is the amount of change from an initial level of some measure of performance [typically measured in either percent change or in decibels (dB)]. This is why the paths in Figure 2 are shown starting at the same point. This adjustment is useful when the corresponding failure times, defined by the amount of change, have more practical value and/or have less relative variability.

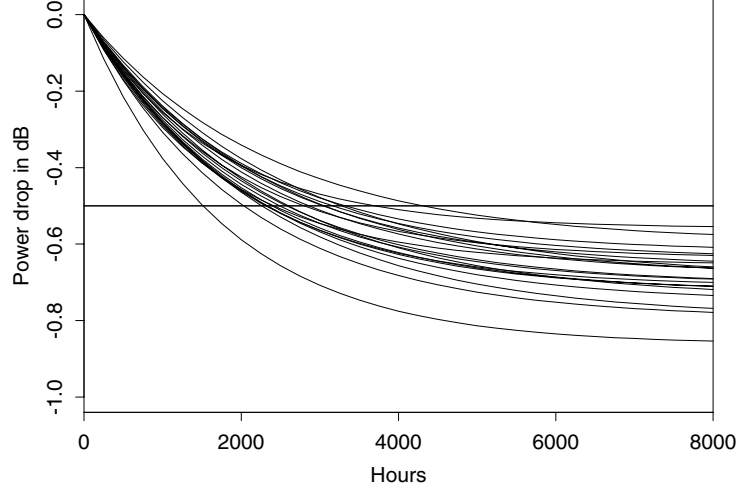


Figure 2: Plot of simulated power degradation with unit-to-unit variability in the power level asymptote  $A_2(\infty)$  and degradation rate  $k_1$ .

### 2.3 General degradation path model

We denote the true degradation path of a particular unit (a function of time) by  $\mathcal{D}(t), t > 0$ . In applications, values of  $\mathcal{D}(t)$  are sampled at discrete points in time,  $t_1, t_2, \dots$ . The observed sample degradation path for unit  $i$  at time  $t_{ij}$  is a unit's actual degradation path plus error and is given by

$$y_{ij} = \mathcal{D}_{ij} + \epsilon_{ij}, \quad i = 1, \dots, n, \quad j = 1, \dots, m_i \quad (3)$$

where  $\mathcal{D}_{ij} = \mathcal{D}(t_{ij}, \beta_i)$  is the actual path for unit  $i$  at time  $t_{ij}$  (the times need not be the same for all units),  $\epsilon_{ij} \sim N(0, \sigma_\epsilon^2)$  is a deviation from the assumed model for unit  $i$  at time  $t_{ij}$ , and  $\beta_i = (\beta_{1i}, \dots, \beta_{ki})$  is a vector of  $k$  unknown parameters for unit  $i$ . The deviations are used to describe measurement error. The total number of inspections on unit  $i$  is denoted by  $m_i$ . Time  $t$  could be real-time, operating time, or some surrogate like miles for automobile tires or loading cycles in fatigue tests. Typically sample paths are described by a model with  $k = 1, 2, 3$  or  $4$  parameters. As described in Section 2.2, some of the parameters in  $\beta$  will be random from unit-to-unit. One or more of the parameters in  $\beta$  could, however, be modeled as constant across all units.

The scales of  $y$  and  $t$  can be chosen (as suggested by physical theory and the data) to simplify the form of  $\mathcal{D}(t, \beta)$ . For example, the relationship between the logarithm of degradation and the logarithm of time might be modeled by the additive relationship in (3). The choice of a degradation model requires not only specification of the form of the  $\mathcal{D}(t, \beta)$  function, but also specification of which of the parameters in  $\beta$  are random and which are fixed and the joint distribution of the random components in  $\beta$ . Lu and Meeker (1993) describe the use of a general family of transformations to a multivariate normal

distribution with mean vector  $\boldsymbol{\mu}_\beta$  and covariance matrix  $\Sigma_\beta$ . For many problems, the Box-Cox family of transformations (Box and Cox 1964) will be useful. In our application we use the log transformation, a special case of the Box-Cox transformation. For fixed parameters in  $\boldsymbol{\beta}$ , it is notationally convenient to set the elements in the corresponding rows and columns in  $\Sigma_\beta$  equal 0.

It is generally reasonable to assume that the random components of the vector  $\boldsymbol{\beta}$  are independent of the  $\epsilon_{ij}$  deviations. We also assume that the  $\epsilon_{ij}$  deviations are independent and identically distributed for  $i = 1, \dots, n$  and  $j = 1, \dots, m_i$ . Because the  $y_{ij}$  are taken serially on a unit, however, there is potential for autocorrelation among the  $\epsilon_{ij}, j = 1, \dots, m_i$ , especially if there are many closely-spaced readings. In many practical applications involving inference on the degradation of units from a population or process, however, if the model fit is good and if the testing and measurement processes are in control, then autocorrelation is typically weak and, moreover, dominated by the unit-to-unit variability in the  $\boldsymbol{\beta}$  values and thus can be ignored. Also, it is well known (e.g., pages 246-249 of Johnston 1972) that point estimates of regression curves are not seriously affected by autocorrelation, but ignoring autocorrelation can result in standard errors that are seriously incorrect. This, however, is not a problem when (as we do) confidence intervals are constructed by using an appropriate simulation-based bootstrap method. In more complicated situations it may also happen that  $\sigma_\epsilon$  will depend on the level of the acceleration variable. Often, however, appropriate modeling (e.g., transformation of the degradation response) will allow the use of a simpler constant- $\sigma_\epsilon$  model.

### 3 Models Relating Degradation and Failure

#### 3.1 Soft failures: specified degradation level

For some products there is a gradual loss of performance (e.g., decreasing light output from a fluorescent light bulb). Then failure would be defined (in a somewhat arbitrary manner) at a specified level of degradation such as 60% of initial output. We call this a “soft failure” definition. See Tseng, Hamada, and Chiao (1995) for an example.

We use  $\mathcal{D}_f$  to denote the critical level for the degradation path above (or below) which failure is assumed to have occurred. The failure time  $T$  is defined as the time when the actual path  $\mathcal{D}(t)$  crosses the critical degradation level  $\mathcal{D}_f$ . Inferences are desired on the failure-time distribution of a particular product or material. For soft failures, it is usually possible to continue observation beyond  $\mathcal{D}_f$ .

#### 3.2 Hard failures: joint distribution of degradation and failure level

For some products, the definition of the failure event is clear—the product stops working (e.g., when the resistance of a resistor deviates too much from its nominal value, causing the oscillator in an electronic circuit to stop oscillating or when an incandescent light bulb burns out). These are called “hard failures.” With hard failures, failure times will not, in general, correspond exactly with a particular level of degradation (like the horizontal line shown in Figure 2). Instead, the level of degradation at which failure (i.e., loss of functionality) occurs will be random from unit to unit and even over time. This could be

modeled by using a distribution to describe unit-to-unit variability in  $\mathcal{D}_f$  or, more generally, the joint distribution of  $\beta$  and the stochastic behavior in  $\mathcal{D}_f$ .

## 4 Acceleration Model

In order to obtain timely information from laboratory tests, it is often possible to use some form of acceleration. Increasing the level of acceleration variables like temperature, humidity, voltage, or pressure can accelerate the chemical or other degradation processes related to specific failure mechanisms such as the weakening of an adhesive mechanical bond or the growth of a conducting filament through an insulator. If an adequate physically-based statistical model is available to relate failure time to levels of accelerating variables, the model can be used to estimate lifetime or degradation rates at product use conditions.

### 4.1 Elevated temperature acceleration

The *Arrhenius* model describing the effect that temperature has on the rate of a simple first-order chemical reaction is

$$\mathcal{R}(\mathbf{temp}) = \gamma_0 \exp \left[ \frac{-E_a}{k_B \times (\mathbf{temp} + 273.15)} \right] = \gamma_0 \exp \left( \frac{-E_a \times 11605}{\mathbf{temp} + 273.15} \right)$$

where  $\mathbf{temp}$  is temperature in  $^{\circ}\text{C}$  and  $k_B = 1/11605$  is Boltzmann's constant in units of electron volts per  $^{\circ}\text{C}$ . The pre-exponential factor  $\gamma_0$  and the reaction activation energy  $E_a$  in units of electron volts are characteristics of the particular chemical reaction. Taking the ratio of the reaction rates at temperatures  $\mathbf{temp}$  and  $\mathbf{temp}_U$  cancels  $\gamma_0$  giving an *Acceleration Factor*

$$\mathcal{AF}(\mathbf{temp}, \mathbf{temp}_U, E_a) = \frac{\mathcal{R}(\mathbf{temp})}{\mathcal{R}(\mathbf{temp}_U)} = \exp \left[ E_a \left( \frac{11605}{\mathbf{temp}_U + 273.15} - \frac{11605}{\mathbf{temp} + 273.15} \right) \right] \quad (4)$$

that depends only on the two temperature levels and the activation energy. If  $\mathbf{temp} > \mathbf{temp}_U$ , then  $\mathcal{AF}(\mathbf{temp}, \mathbf{temp}_U, E_a) > 1$ . For simplicity, we use the notation  $\mathcal{AF}(\mathbf{temp}) = \mathcal{AF}(\mathbf{temp}, \mathbf{temp}_U, E_a)$  when  $\mathbf{temp}_U$  and  $E_a$  are understood to be, respectively, product use (or other specified base-line) temperature and a reaction-specific activation energy.

### 4.2 Nonlinear degradation path and reaction-rate acceleration

Consider the simple chemical degradation path model from Example 2, rewritten in the generic notation and with a temperature acceleration factor affecting the rate of the reaction:

$$\mathcal{D}(t; \mathbf{temp}) = \mathcal{D}_{\infty} \times \{1 - \exp[-\mathcal{R}_U \times \mathcal{AF}(\mathbf{temp}) \times t]\}. \quad (5)$$

Here  $\mathcal{R}_U$  is the rate reaction at use temperature  $\mathbf{temp}_U$ ,  $\mathcal{R}_U \times \mathcal{AF}(\mathbf{temp})$  is the rate reaction at temperature  $\mathbf{temp}$ , and  $\mathcal{D}_{\infty}$  is the asymptote. When degradation is measured on a scale decreasing from zero,  $\mathcal{D}_{\infty} < 0$  and we specify that failure occurs at the smallest  $t$  such that  $\mathcal{D}(t) \leq \mathcal{D}_f$ . Figure 3 shows model (5) for fixed values of  $\mathcal{R}_U$ ,  $\mathcal{D}_{\infty}$ , and  $E_a$  for 4 different

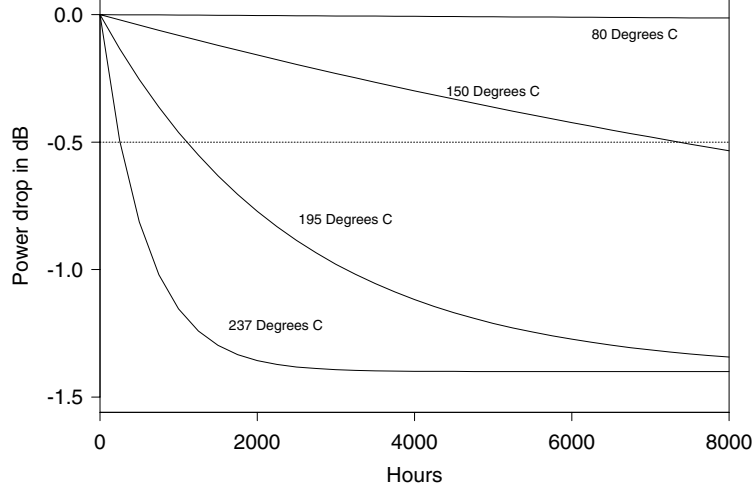


Figure 3: Illustration of the effect of Arrhenius temperature dependence on the degradation caused by a single-step chemical reaction.

levels of temperature. Equating  $\mathcal{D}(T; \mathbf{temp})$  to  $\mathcal{D}_f$  and solving for  $T$  gives the failure time at temperature  $\mathbf{temp}$  as

$$T(\mathbf{temp}) = \frac{-\frac{1}{\mathcal{R}_U} \log\left(1 - \frac{\mathcal{D}_f}{\mathcal{D}_\infty}\right)}{\mathcal{AF}(\mathbf{temp})} = \frac{T(\mathbf{temp}_U)}{\mathcal{AF}(\mathbf{temp})} \quad (6)$$

where  $T(\mathbf{temp}_U) = -\frac{1}{\mathcal{R}_U} \log\left(1 - \frac{\mathcal{D}_f}{\mathcal{D}_\infty}\right)$  is failure time at use conditions.

The right-hand side of (6) shows that the life/temperature model induced by this simple degradation process and the Arrhenius-acceleration model results in a Scale Accelerated Failure Time (SAFT) model. Under the SAFT model, the degradation path (and thus a corresponding failure event) for a unit at any temperature can be used to determine the degradation path (and failure time) that the same unit would have had at any other specified temperature, simply by scaling the time axis by the acceleration factor  $\mathcal{AF}(\mathbf{temp})$ . Failure-time models are scaled similarly. For example, if  $T(\mathbf{temp}_U)$ , the failure time at use temperature, has a Weibull distribution with scale parameter  $\alpha_U$  and shape parameter  $\beta$  [denoted by  $T(\mathbf{temp}_U) \sim \text{WEIB}(\alpha_U, \beta)$ ], then failure time at other temperatures is distributed  $T(\mathbf{temp}) \sim \text{WEIB}[\alpha_U/\mathcal{AF}(\mathbf{temp}), \beta]$ . Similarly, if  $T(\mathbf{temp}_U)$  has a lognormal distribution with scale parameter  $\exp(\mu_U)$  and shape parameter  $\sigma$  [denoted by  $T(\mathbf{temp}_U) \sim \text{LOGNOR}(\mu_U, \sigma)$ ], then  $T(\mathbf{temp}) \sim \text{LOGNOR}[\mu_U - \log(\mathcal{AF}(\mathbf{temp})), \sigma]$ . In general a model will be SAFT if the failure mechanism is governed by a single-step chemical reaction with a rate that depends on an acceleration variable like temperature but is otherwise constant over time. Klinger (1992) also notes this relationship.

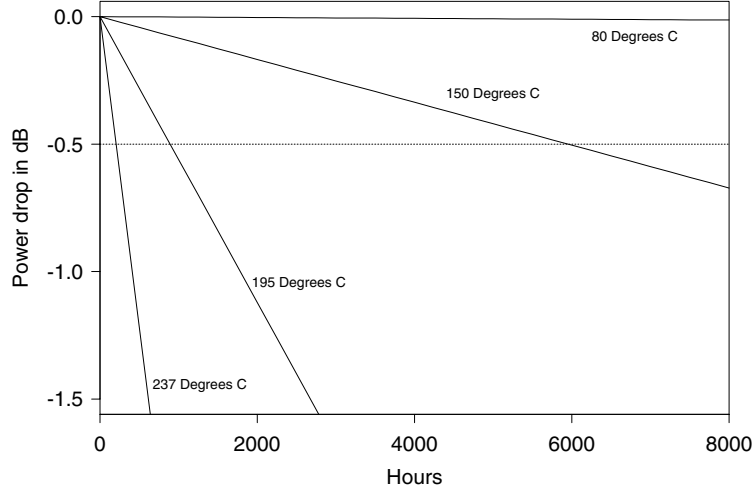


Figure 4: Illustration of the effect of Arrhenius temperature dependence on a linear degradation process.

### 4.3 Linear degradation path reaction-rate acceleration

Consider model (5) along with the critical level  $\mathcal{D}_f$ . For values of  $t$  such that  $\mathcal{D}(t)$  is small relative to  $\mathcal{D}_\infty$ ,

$$\begin{aligned} \mathcal{D}(t; \text{temp}) &= \mathcal{D}_\infty \times \{1 - \exp[-\mathcal{R}_U \times \mathcal{A}\mathcal{F}(\text{temp}) \times t]\} \\ &\approx \mathcal{D}_\infty \times \mathcal{R}_U \times \mathcal{A}\mathcal{F}(\text{temp}) \times t = \mathcal{R}_U^+ \times \mathcal{A}\mathcal{F}(\text{temp}) \times t \end{aligned} \quad (7)$$

is approximately linear in time  $t$  with slope  $\mathcal{R}_U^+ \times \mathcal{A}\mathcal{F}(\text{temp})$  where  $\mathcal{R}_U^+ = \mathcal{D}_\infty \times \mathcal{R}_U$ . Also some degradation processes (e.g., automobile tire wear) are naturally linear in time. Figure 4 shows model (7) for fixed values of  $\mathcal{R}_U^+$  and  $E_a$  for 4 different values of temperature.

If failure occurs when  $\mathcal{D}(T) \leq \mathcal{D}_f$ , we can equate  $\mathcal{D}(T; \text{temp})$  to  $\mathcal{D}_f$  and solve for  $T$  to give the failure time as

$$T(\text{temp}) = \frac{\mathcal{D}_f}{\mathcal{R}_U^+} \times \frac{1}{\mathcal{A}\mathcal{F}(\text{temp})} = \frac{T(\text{temp}_U)}{\mathcal{A}\mathcal{F}(\text{temp})}$$

where  $T(\text{temp}_U) = \mathcal{D}_f / \mathcal{R}_U^+$  is failure time at use conditions. Thus this is also an SAFT model.

### 4.4 Degradation with parallel reactions

Consider a more complicated degradation path model with two parallel one-step failure-causing chemical reactions leading to

$$\begin{aligned} \mathcal{D}(t; \text{temp}) &= \mathcal{D}_{1\infty} \times \{1 - \exp[-\mathcal{R}_{1U} \times \mathcal{A}\mathcal{F}_1(\text{temp}) \times t]\} \\ &+ \mathcal{D}_{2\infty} \times \{1 - \exp[-\mathcal{R}_{2U} \times \mathcal{A}\mathcal{F}_2(\text{temp}) \times t]\}. \end{aligned}$$

Here  $\mathcal{R}_{1U}$  and  $\mathcal{R}_{2U}$  are the use-condition rates of the two parallel reactions contributing to failure. Suppose that temperature dependence for each reaction rate can be described, individually, by the Arrhenius acceleration factors  $\mathcal{AF}_1(\mathbf{temp})$  and  $\mathcal{AF}_2(\mathbf{temp})$ , respectively. Unless  $\mathcal{AF}_1(\mathbf{temp}) = \mathcal{AF}_2(\mathbf{temp})$  for all  $\mathbf{temp}$ , this degradation model does *not* lead to an SAFT model. Intuitively, this is because temperature affects the degradation processes differently, inducing a nonlinearity into the acceleration function relating times at two different temperatures. To obtain useful extrapolative models it is, in general, necessary to have models for the important individual degradation processes.

#### 4.5 Accelerated degradation model parameters

Our model's rate-acceleration parameters are unknown fixed-effects parameters (e.g., in the Arrhenius model we assume no unit-to-unit variability in activation energy  $E_a$ ). As described in Section 2.3, fixed-effects parameters are included, notationally, in the parameter vector  $\beta$  introduced in Section 2.3. Thus for the single-step models in Sections 4.2 and 4.3, we have one additional parameter to estimate. The total number of parameters in  $\beta$  for an individual unit, is still denoted by  $k$ .

The values of  $\beta$  corresponding to individual units may be of interest in some applications (e.g., to predict the future degradation of a particular unit, based on a few early readings). Subsequent development in this paper, however, will concentrate on the use of degradation data to make inferences about the population or process from which the sample units were obtained or predictions about the failure-time distribution at specific levels of the accelerating variable (e.g., temperature) of future units from the process. In this case, the underlying model parameters are  $\mu_\beta$  and  $\Sigma_\beta$ , as well as the standard deviation  $\sigma_\epsilon$ . Again, the appropriate rows and columns in  $\Sigma_\beta$ , corresponding to the fixed parameters in  $\beta$ , contain 0's. For shorthand, we will use  $\theta_\beta = (\mu_\beta, \Sigma_\beta)$  to denote the parameters of the overall degradation population or process.

**Example 3 Device-B power output degradation model parameterization.** For the Device-B power-drop data in Example 1, the scientists responsible for the product were confident that degradation was caused by a simple one-step chemical reaction that could be described by the model in Example 2. Thus for the data in Figure 1, we will use the accelerated degradation model in (5), assuming that  $\mathcal{R}_U$  and  $\mathcal{D}_\infty$  are random from unit to unit. Then a possible parameterization would be  $(\beta_1, \beta_2, \beta_3) = [\log(\mathcal{R}_U), \log(-\mathcal{D}_\infty), E_a]$  where the first two parameters are random effects and activation energy  $E_a$  is a fixed effect. That is,  $E_a$  is assumed to be a material property that does not depend on temperature and that is constant from unit to unit. The log transformation on  $\mathcal{R}_U$  and  $-\mathcal{D}_\infty$  is consistent with the data and assures that the model for the random effects is consistent with the physical model for degradation (in terms of the signs of  $\mathcal{R}_U$  and  $-\mathcal{D}_\infty$ ). ■

## 5 Estimation of Accelerated Degradation Model Parameters

Lu and Meeker (1993) used a two-stage method to estimate the parameters of the mixed-effects accelerated degradation model in (5). The methods developed by Lindstrom and Bates (1990) and Pinheiro and Bates (1995a) provide excellent, computationally efficient

approximations to ML estimates. The software implementation in Pinheiro and Bates (1995b), also available in S-Plus, has made the methods easy to use. Indeed, we have found, in some cases, that doing an approximate ML is faster than doing the  $n$  nonlinear least squares estimations required for the two-state method. ML estimation also has the advantages of desirable large-sample properties and the ability to easily use sample paths for which all of the parameters cannot be estimated (as is the case in our example where the assumed model cannot be fit to the 150°C).

The two-stage estimation method is useful for getting starting values for the ML approach or for modeling, especially, when consideration is given to something other than a joint normal distribution for the random effects.

The likelihood for the mixed-effect accelerated degradation model in Section 4 can be expressed as

$$L(\boldsymbol{\mu}_\beta, \Sigma_\beta, \sigma_\epsilon | \text{DATA}) = \prod_{i=1}^n \int_{-\infty}^{\infty} \cdots \int_{-\infty}^{\infty} \left[ \prod_{j=1}^{m_i} \frac{1}{\sigma_\epsilon} \phi(\zeta_{ij}) \right] f_\beta(\boldsymbol{\beta}_i; \boldsymbol{\mu}_\beta, \Sigma_\beta) d\beta_{1i}, \dots, d\beta_{ki} \quad (8)$$

where  $\zeta_{ij} = [y_{ij} - \mathcal{D}(t_{ij}, \boldsymbol{\beta}_i)] / \sigma_\epsilon$ ,  $\phi(z)$  is the standard normal density function, and  $f_\beta(\boldsymbol{\beta}_i; \boldsymbol{\mu}_\beta, \Sigma_\beta)$  is the multivariate normal distribution density function. See Palmer, Phillips and Smith (1991) for motivation and explanation. To simplify notation and presentation, we continue to collect both the unit-to-unit random effects and fixed effects parameters into the vector  $\boldsymbol{\beta}_i$  with the entries in  $\Sigma_\beta$  being 0 for the rows and columns corresponding to the fixed effects.

Evaluation of (8) will, in general, require numerical approximation of  $n$  integrals of dimension  $k_r$  (where  $n$  is the number of paths and  $k_r \leq k$  is the number of random parameters in each path). Maximizing (8) with respect to  $(\boldsymbol{\mu}_\beta, \Sigma_\beta, \sigma_\epsilon)$  directly, even with today's computational capabilities, is extremely difficult unless  $\mathcal{D}(t)$  is a linear function. Pinheiro and Bates (1995a) describe and compare estimation schemes that provide approximate maximum likelihood estimates of  $\boldsymbol{\theta}_\beta = (\boldsymbol{\mu}_\beta, \Sigma_\beta)$  and  $\sigma_\epsilon$ , as well as estimates of the random unit-specific components in  $\boldsymbol{\beta}_i, i = 1, \dots, n$ . Pinheiro and Bates (1995b) implement a modification of the method of Lindstrom and Bates (1990). The examples in this paper were computed with the Pinheiro and Bates (1995b) program and some other complementary S-Plus functions that were written specifically for accelerated degradation data analysis.

**Example 4 Estimates of Device-B model parameters.** Continuing with Example 3, we fit model (5) using S-plus function `nlme`. To improve the stability and robustness of the approximate ML algorithm, it is important to reduce the correlation between the estimates of  $E_a$  and the parameters relating to the reaction rate  $\mathcal{R}$ . Thus it is preferable to estimate  $\mathcal{R}$  at some level of temperature that is central to the experimental temperatures, rather than the use-temperature. We use 195°C and parameterize with  $\beta_1 = \log[\mathcal{R}(195)]$ ,  $\beta_2 = \log(-\mathcal{D}_\infty)$ , and  $\beta_3 = E_a$  where  $\mathcal{R}(195) = \mathcal{R}_U \times \mathcal{AF}(195)$  is the reaction rate at 195°C. Our model assumes that  $(\beta_1, \beta_2)$  has a bivariate normal distribution from unit-to-unit and that  $\beta_3 = E_a$  is a constant, but unknown, material property. S-plus function `nlme` gives the following approximate ML estimates of the mixed-effect model parameters

$$\hat{\boldsymbol{\mu}}_\beta = \begin{pmatrix} -7.572 \\ .3510 \\ .6670 \end{pmatrix}, \quad \hat{\Sigma}_\beta = \begin{pmatrix} .15021 & -.02918 & 0 \\ -.02918 & .01809 & 0 \\ 0 & 0 & 0 \end{pmatrix}$$

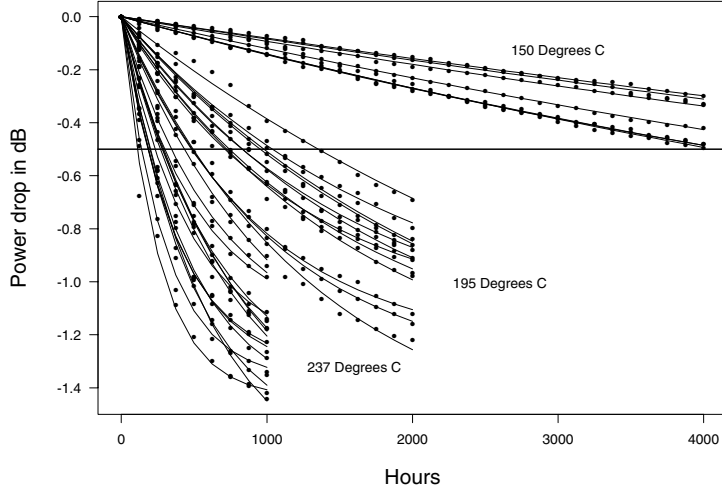


Figure 5: Device-B power drop observations and fitted degradation model for the 34 sample paths.

and  $\hat{\sigma}_\epsilon = .0233$ . Figure 5 shows the fitted model (5) for each of the sample paths (indicated by the points on the plot) for the Device-B degradation data. Figure 6 plots the estimates of the  $\beta_1, \beta_2$  parameters for each of the 34 sample paths, indicating the reasonableness of the bivariate normal distribution model for this random-coefficients model. ■

## 6 Evaluation and estimation of $F(t)$

For the remainder of this paper we will assume that  $\mathcal{D}_f$  is a constant. Allowing  $\mathcal{D}_f$  to be random is a computationally straightforward generalization but would complicate the presentation.

For a specified degradation model, the distribution function of  $T$ , the crossing (or failure) time, can be written as a function of the degradation model parameters and  $\mathcal{D}_f$ . In particular, a unit fails by time  $t$  if degradation level reaches  $\mathcal{D}_f$  by time  $t$ . Thus, in Figure 5,

$$\Pr(T \leq t) = F(t) = F(t; \boldsymbol{\theta}_\beta) = \Pr[\mathcal{D}(t, \boldsymbol{\beta}) \leq \mathcal{D}_f]. \quad (9)$$

That is, the distribution of  $T$  depends on the distribution of  $\boldsymbol{\beta}$  and the distribution of the  $\boldsymbol{\beta}$  depends on the basic path parameters in  $\boldsymbol{\theta}_\beta$ .

### 6.1 Analytical expressions for $F(t)$

For some particularly simple path models,  $F(t)$  can be expressed as a function of the basic path parameters in a closed form. With acceleration,  $F(t)$  also depends on the level of acceleration variables like temperature. As illustrated in Section 3.1, one or more of the

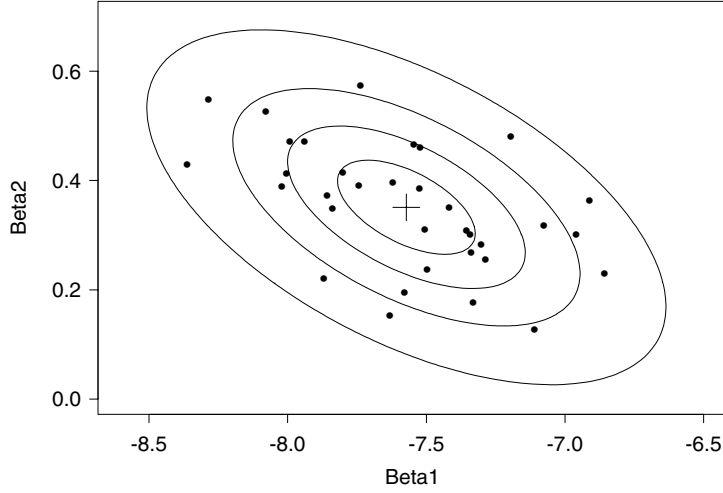


Figure 6: Plot of  $\widehat{\beta}_{1i}$  versus  $\widehat{\beta}_{2i}$  for the  $i = 1, \dots, 34$  sample paths from Device-B, also showing contours corresponding to the fitted bivariate normal distribution. The + marks the estimates of the means of  $\beta_1$  and  $\beta_2$ .

elements in  $\beta$  may be expressed as a function of accelerating variables, but notation for this dependency will be suppressed until needed.

**Example 5 Linear degradation with lognormal rate.** Suppose failure occurs when  $\mathcal{D}(t) \geq \mathcal{D}_f$  and that the actual degradation path of a particular unit is given by

$$\mathcal{D}(t) = \beta_1 + \beta_2 t$$

where  $\beta_1 < \mathcal{D}_f$  is fixed and  $\beta_2 > 0$  varies from unit to unit according to a LOGNOR( $\mu, \sigma$ ) distribution. This implies that

$$\Pr(\beta_2 \leq b) = \Phi \left[ \frac{\log(b) - \mu}{\sigma} \right]$$

where  $\Phi(z)$  is the standard normal cdf and  $\mu$  and  $\sigma$  are, respectively, the mean and standard deviation of  $\log(\beta_2)$ .

The parameter  $\beta_1$  represents the common initial amount of degradation of all the test units at time 0 and  $\beta_2$  represents the degradation rate, random from unit-to-unit. Then

$$\begin{aligned} F(t; \beta_1, \mu, \sigma) &= \Pr(\mathcal{D}(t) \geq \mathcal{D}_f) = \Pr(\beta_1 + \beta_2 t \geq \mathcal{D}_f) = \Pr\left(\beta_2 \geq \frac{\mathcal{D}_f - \beta_1}{t}\right) \\ &= 1 - \Phi \left[ \frac{\log(\mathcal{D}_f - \beta_1) - \log(t) - \mu}{\sigma} \right] = \Phi \left[ \frac{\log(t) - [\log(\mathcal{D}_f - \beta_1) - \mu]}{\sigma} \right], \quad t > 0. \end{aligned}$$

This shows that  $T$  has a lognormal distribution with parameters that depend on the basic path parameters  $\theta_\beta = (\beta_1, \mu, \sigma)$ , and  $\mathcal{D}_f$ . That is,  $\exp[\log(\mathcal{D}_f - \beta_1) - \mu]$  is the lognormal median and  $\sigma$  is the lognormal shape parameter. ■

See Section 2.3 of Lu and Meeker (1993) for some other examples.

## 6.2 Numerical evaluation of $F(t)$

For most practical path models, especially when  $\mathcal{D}(t)$  is nonlinear and more than one of the elements in  $\boldsymbol{\beta} = (\beta_1, \dots, \beta_k)$  is random, it may be necessary to evaluate  $F(t)$  numerically. For two random variables (say  $\beta_1$  and  $\beta_2$ ), the following algorithm provides a simple means of doing this.

**Algorithm 1 Evaluation of  $F(t)$  by direct integration.** To use this algorithm it is necessary that  $\mathcal{D}(t)$  be a monotone function of one of the parameters (say  $\beta_2$ ) for a fixed value of  $\beta_1$ . Then if  $(\beta_1, \beta_2)$  has a bivariate normal distribution with parameters  $\boldsymbol{\theta}_\beta = (\mu_{\beta_1}, \mu_{\beta_2}, \sigma_{\beta_1}^2, \sigma_{\beta_2}^2, \rho)$ ,

$$F(t) = P(T \leq t) = \int_{-\infty}^{\infty} \Phi \left[ -\frac{g(\mathcal{D}_f, t, \beta_1) - \mu_{\beta_2|\beta_1}}{\sigma_{\beta_2|\beta_1}} \right] \frac{1}{\sigma_{\beta_1}} \phi \left( \frac{\beta_1 - \mu_{\beta_1}}{\sigma_{\beta_1}} \right) d\beta_1$$

where  $g(\mathcal{D}_f, t, \beta_1)$  is the value of  $\beta_2$  that gives  $\mathcal{D}(t) = \mathcal{D}_f$  for specified  $\beta_1$  and where

$$\begin{aligned} \mu_{\beta_2|\beta_1} &= \mu_{\beta_2} + \rho\sigma_{\beta_2} \left( \frac{\beta_1 - \mu_{\beta_1}}{\sigma_{\beta_1}} \right) \\ \sigma_{\beta_2|\beta_1}^2 &= \sigma_{\beta_2}^2 (1 - \rho^2). \end{aligned}$$

In principle, this approach can be extended in a straightforward manner when there are more than 2 continuous random variables. The amount of computational time needed to evaluate the multidimensional integral will, however, increase exponentially with the dimension of the integral. ■

## 6.3 Monte Carlo evaluation of $F(t)$

Monte Carlo simulation, as illustrated in Figure 2, is a particularly versatile method for evaluating  $F(t)$ . Evaluation is done by generating a large number of random sample paths from the assumed path model. Then the proportion of paths crossing  $\mathcal{D}_f$  by time  $t$  provides an evaluation of  $F(t)$ . This approach is described in detail and illustrated in Section 4.1 of Lu and Meeker (1993).

## 6.4 Estimation of $F(t)$

One can estimate the failure-time distribution  $F(t)$  by substituting the estimates  $\hat{\boldsymbol{\theta}}_\beta$  into (9) giving

$$\hat{F}(t) = F(t; \hat{\boldsymbol{\theta}}_\beta).$$

This is straightforward for the case when  $F(t)$  can be expressed in a closed form. When there is no closed-form expression for  $F(t)$ , and when numerical transformation methods are too complicated, one can use Algorithm 1 or Monte Carlo simulation to evaluate (9) at  $\hat{\boldsymbol{\theta}}_\beta$ .

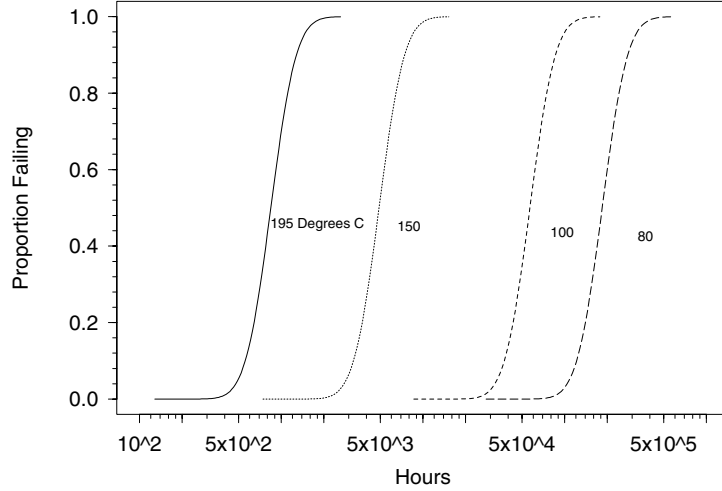


Figure 7: Estimates of the Device-B life distributions at 80, 100, 150, and 195°C, based on the degradation data.

**Example 6 Device-B degradation data estimate of  $F(t)$ .** Figure 7 shows  $\hat{F}(t)$  for Device-B based on the IC power-drop data with failure defined as a power drop of  $\mathcal{D}_f = -0.5$  dB. Estimates are shown for 195°C, 150°C, 100°C, and 80°C. These estimates were computed with Algorithm 1, using the estimates of the model parameters  $\hat{\theta}_\beta = (\hat{\mu}_\beta, \hat{\Sigma}_\beta)$  from Example 4. ■

## 7 Confidence Intervals Based on Bootstrap Sampling

Because there is no simple method of computing standard errors for  $\hat{F}(t)$ , we use a simulation of the sampling/failure process and the bias-corrected percentile bootstrap method, described in Efron (1985), to obtain parametric bootstrap confidence intervals for quantities of interest. The bias-corrected percentile bootstrap method for obtaining confidence intervals for  $F(t)$  at a specified temperature is implemented with the following algorithm.

**Algorithm 2 Bootstrap confidence intervals from degradation data.**

1. Use the observed data from the  $n$  sample paths to compute the estimates  $\hat{\theta}_\beta$  and  $\hat{\sigma}_\epsilon$ .
2. Use Algorithm 1 or Monte Carlo simulation with  $\hat{\theta}_\beta$  as input to compute the estimate  $\hat{F}(t)$  at desired values of  $t$ .
3. Generate a large number (e.g.,  $B = 4,000$ ) of bootstrap samples and corresponding bootstrap estimates  $\hat{F}^*(t)$  according to the following steps.
  - (a) Generate  $n$  simulated realizations of the random path parameters  $\beta_i^*, i = 1, \dots, n$ , each from a multivariate normal distribution with parameters  $\hat{\theta}_\beta$ .

- (b) Using the same sampling scheme as in the original experiment, compute  $n$  simulated observed paths from

$$y_{ij}^* = \mathcal{D}(t_{ij}; \beta_i^*) + \epsilon_{ij}^*$$

up to the planned stopping time  $t_{c_i}$ , where the  $\epsilon_{ij}^*$  values are independent simulated deviations generated from  $N(0, \hat{\sigma}_\epsilon^2)$  and  $t_{c_i}$  is the fixed censoring time for the unit  $i$ .

- (c) Use the  $n$  simulated paths to estimate parameters of the path model, giving the bootstrap estimates  $\hat{\theta}_\beta^*$
4. Use Algorithm 1 or Monte Carlo simulation with  $\hat{\theta}_\beta^*$  as input to compute the bootstrap estimates  $\hat{F}^*(t)$  at desired values of  $t$ .
5. For each desired value of  $t$ , the bootstrap confidence interval for  $F(t)$  is computed using the following steps
- (a) Sort the  $B$  values  $\hat{F}^*(t)_1, \dots, \hat{F}^*(t)_B$  in increasing order giving  $\hat{F}^*(t)_{[b]}$ ,  $b = 1, \dots, B$ .
- (b) Following Efron (1985), the lower and upper bounds of pointwise approximate  $100(1 - \alpha)\%$  confidence intervals for the distribution function  $F(t)$  are

$$\left[ \underline{F}(t), \tilde{F}(t) \right] = \left[ \hat{F}^*(t)_{[lB]}, \hat{F}^*(t)_{[uB]} \right]$$

where

$$l = \Phi \left[ 2\Phi^{-1}(q) + \Phi^{-1}(\alpha/2) \right], \quad u = \Phi \left[ 2\Phi^{-1}(q) + \Phi^{-1}(1 - \alpha/2) \right],$$

$\Phi^{-1}(p)$  is the standard normal  $p$  quantile, and  $q$  is the proportion of the  $B$  values of  $\hat{F}^*(t)$  that are less than  $\hat{F}(t)$ . Setting  $q = .5$  gives the percentile bootstrap method.

For an SAFT model, once  $\hat{F}^*(t)$  has been computed in step 4 for one set of conditions for the accelerating variable, it is possible to obtain  $\hat{F}^*(t)$  for other conditions by simply scaling times. Otherwise the results in step 3 need to be reused in step 4 to recompute the  $\hat{F}^*(t)$  values for each new set of conditions. ■

**Example 7 Degradation data bootstrap confidence intervals for  $F(t)$ .** Continuing with Example 6, Figure 8 shows the point estimate and a set of pointwise two-sided approximate 90% and 80% bootstrap bias-corrected percentile confidence intervals for  $F(t)$  at 80°C, based on the IC power-drop data with failure defined as a power drop of  $\mathcal{D}_f = -.5\text{dB}$ . The bootstrap confidence intervals were computed by using Algorithm 1 and Algorithm 2 to evaluate  $\hat{F}^*(t)$ . Specifically, the point estimate for  $F(t)$  at 130 thousand hours is .14 and the approximate 90% confidence interval is [.005, .64]. The extremely wide interval is due to the small number of units tested at 150°C and the large amount of extrapolation required to estimate to  $F(t)$  at 80°C. ■

If there is appreciable autocorrelation in the  $\epsilon_{ij}$ , then the  $\epsilon_{ij}^*$  values in step 3b of Algorithm 2 should be generated from an estimated autoregressive model, as described in Chapter 9 of Shao and Tu (1995).

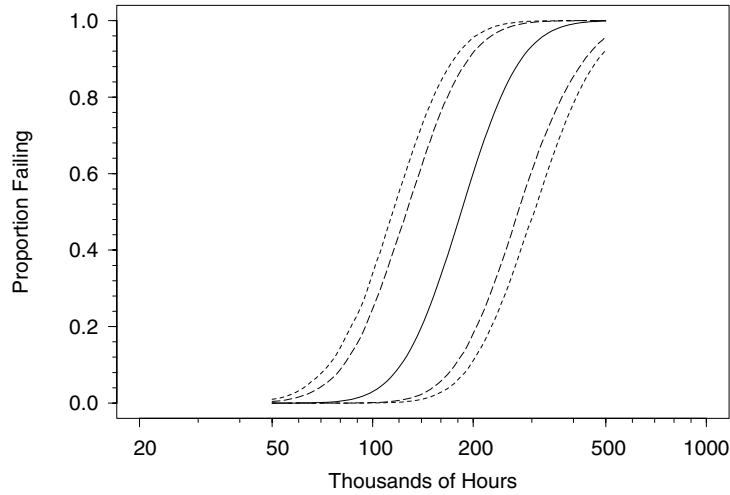


Figure 8: Estimates of the Device-B life distribution at 80°C with approximate 80% and 90% pointwise two-sided bootstrap confidence intervals based on the IC power-drop data with failure defined as a power drop of  $\mathcal{D}_f = -.5\text{dB}$ .

## 8 Comparison with Traditional Accelerated Life Test Analyses

This section compares accelerated degradation and accelerated life test analyses. With failure defined as power drop below  $-.5\text{ dB}$ , there were no failures at 150°C. Although it is possible to fit a model to the resulting life data, the degree of extrapolation with no failures at 150°C would be, from a practical point of view, unacceptable. The comparison will be useful for showing one of the main advantages of degradation analysis—the ability to use degradation data for units that have not failed to provide important information at lower levels of the accelerating variable where few, if any, failures will be observed, thus reducing the degree of extrapolation.

Figure 9 shows a scatter plot of the failure time data, obtained from the degradation data in Figure 1. Figure 10 is a multiple lognormal probability plot with the straight lines showing individual lognormal distributions fitted to the samples at 237°C and 195°C. This figure shows that the lognormal distributions provide a good fit at both temperatures. Figure 11 is also a multiple lognormal probability plot for the individual samples at 237°C and 195°C. In this case, however, the superimposed lines show the fitted lognormal-Arrhenius model relating the life distributions to temperature. This is a commonly used accelerated life test model for electronic components (e.g., Nelson 1990 and Tobias and Trindade 1995). Under the lognormal-Arrhenius model log failure time has a normal distribution with mean

$$\mu = \beta_0 + \beta_3 \left( \frac{11605}{\text{temp} + 273.15} \right)$$

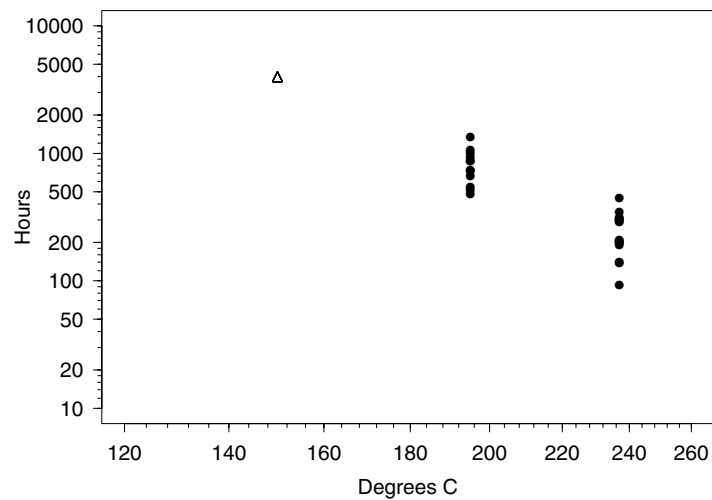


Figure 9: Scatterplot of Device-B failure-time data with failure defined as power drop below  $-0.5$  dB. The symbol  $\Delta$  indicates the 7 units that were tested at  $150^\circ\text{C}$  and had not failed at the end of 4000 hours.

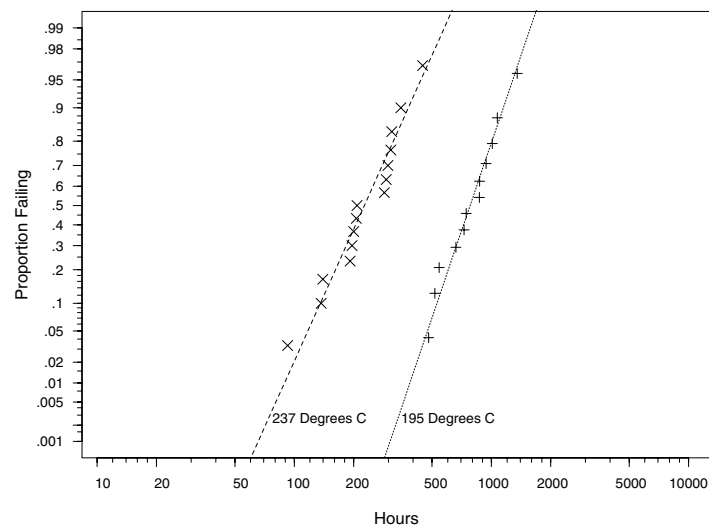


Figure 10: Individual lognormal probability plots of the Device-B failure-time data with failure defined as power drop below  $-0.5$  dB.

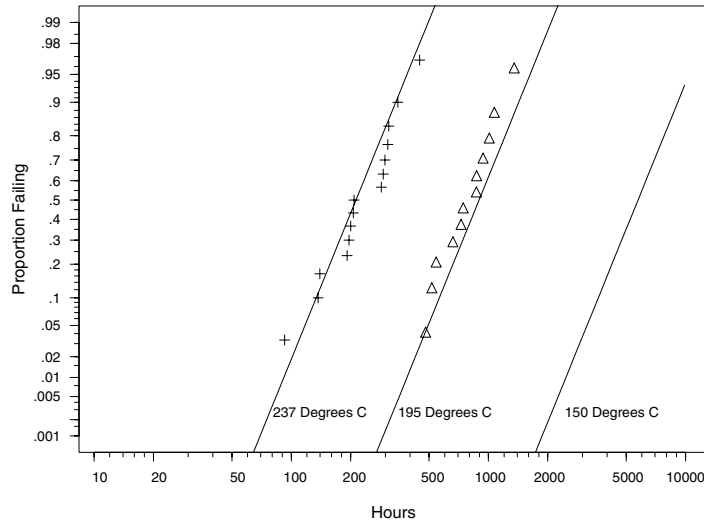


Figure 11: Lognormal-Arrhenius model fit to the Device-B failure-time data with failure defined as power drop below  $-0.5$  dB.

and constant standard deviation  $\sigma_\epsilon$ . In relation to the lognormal-Arrhenius failure-time model described in Section 4.2, the slope  $\beta_3 = E_a$  is the activation energy and the intercept is

$$\beta_0 = \mu_U - \beta_3 \left( \frac{11605}{\text{temp}_U + 273.15} \right).$$

The estimated lognormal cdfs in Figure 11 are parallel because of the constant  $\sigma_\epsilon$  assumption. This plot shows some deviations from the assumed model. These deviations, however, are within what could be expected from random variability alone (a likelihood ratio test comparing the model depicted in Figure 11 with independent ML fits at each level of temperature, shown on Figure 10, had a  $p$ -value of .052).

Figure 12 shows the same lognormal-Arrhenius model fit given in Figure 11 with an extrapolated estimate of the cdf at  $80^\circ\text{C}$ . The dotted lines on this figure are the degradation-model-based estimates of the  $-0.5\text{dB}$ -definition failure-time distributions shown in Figure 7. There are small differences between the lognormal and the degradation models at  $237^\circ\text{C}$  and  $195^\circ\text{C}$ . The difference at  $80^\circ\text{C}$  has been amplified by extrapolation. The degradation estimate would have more credibility because it makes full use of the information available at  $150^\circ\text{C}$ .

The overall close agreement between the degradation model and the lognormal failure-time model can be explained by referring to the models introduced in Section 4.2. There we showed that failure time will follow a lognormal distribution if  $T(\text{temp}_U) = -(1/\mathcal{R}_U) \log(1 - \mathcal{D}_f/\mathcal{D}_\infty)$  follows a lognormal distribution. In our degradation model,  $\log(\mathcal{R}_U)$  and  $\log(-\mathcal{D}_\infty)$  [and thus  $\log(\mathcal{D}_f/\mathcal{D}_\infty)$ ] are assumed to follow a joint normal distribution. If  $\mathcal{D}_f/\mathcal{D}_\infty$  is small relative to 1 (as in this example), then  $\log(1 - \mathcal{D}_f/\mathcal{D}_\infty) \approx -\mathcal{D}_f/\mathcal{D}_\infty$  and thus  $T(\text{temp}_U)$  is

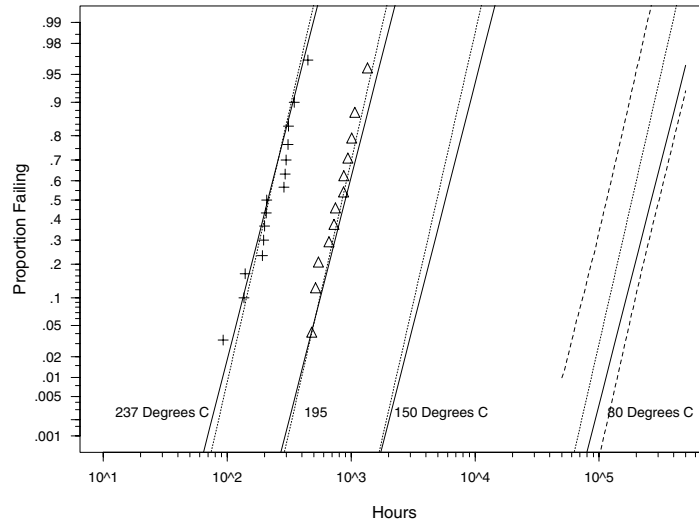


Figure 12: Lognormal-Arrhenius model fit to the Device-B failure-time data with failure defined as power drop below  $-0.5$  dB (solid lines) compared with the corresponding degradation model estimates (dotted lines). Also shown is the set of pointwise approximate 90% bootstrap confidence intervals for  $F(t)$  at  $80^\circ\text{C}$ , based on the degradation analysis.

approximately the ratio of two lognormal random variables, and the ratio of two lognormal random variables also follows a lognormal distribution.

Figure 13 is similar to Figure 12 with a fitted Weibull distribution for failure time. Comparing Figures 12 and 13, the lognormal ALT and degradation models provide a somewhat better fit to the data.

## 9 Concluding Remarks and Areas for Further Research

Using degradation data offers some important advantages for making reliability inferences and predictions, especially when test time is severely limited and few or no failures are expected at lower levels of acceleration variables in an accelerated test. Although degradation analysis requires stronger modeling assumptions (shape of degradation curves and distributions for the random effects), there is better opportunity to assess the adequacy of such assumptions and to combine important physical understanding of failure process with limited, expensive data.

There are a number of important extensions of this work, suggesting areas for future research. These include

- The development of more and better physical/chemical models for failure-causing degradation.
- In some products there may be more than one failure mechanism and thus more than one degradation process with the correspondingly different chemical reactions that

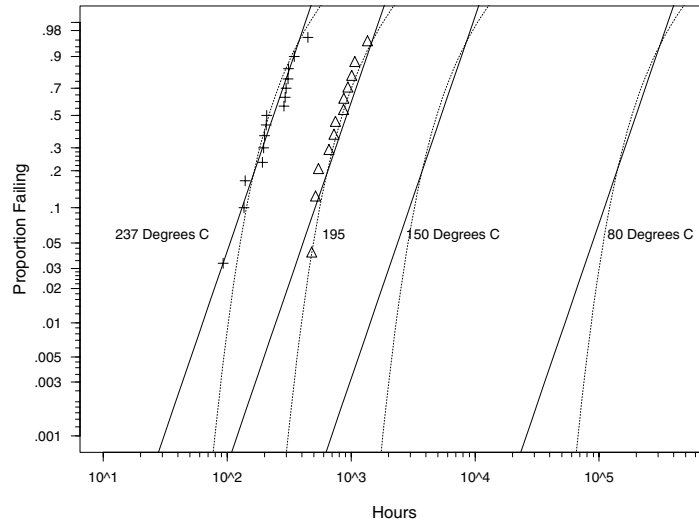


Figure 13: Weibull-Arrhenius model fit to the Device-B failure-time data (solid lines) compared with the degradation model estimates (dotted lines).

may be accelerated at different rates. Physical models and corresponding statistical methods are needed for dealing with such problems.

- Exact ML and likelihood-based methods for inference are computationally burdensome. With continuing increases in computing power, however, such methods could become practicable in the future.
- As explained in Section 2.3, we have assumed that the appropriate transformation (e.g., a Box-Cox transformation) for the random effects parameters is known. The multivariate generalization of the probability-integral transform given in Rosenblatt (1952) suggests the use of more general joint families of distributions for the path parameters.
- It would be possible to include the choice of parameter transformation (e.g., ML estimation of the Box-Cox transformation parameters) as part of the estimation/bootstrap procedure.
- The models in this paper have assumed that given a unit's random parameters, the degradation process is deterministic. Such a model is adequate for many well-behaved failure processes. In some situations, however, additional within-unit or environmental stochastic variability may need to be modeled. For example, Sobczyk and Spencer (1992) describe stochastic process models for fatigue failure.
- Nelson (1995) describes models and analysis methods for problems with random non-zero degradation initiation times. His methods assume destructive inspection so that each sample unit will provide a single (possibly censored) degradation response. It

would be useful to extend this work to allow for multiple readings on individual test units.

## Acknowledgments

We would like to thank the Editor, Associate Editor and the referees for their helpful comments on an earlier version of this paper. Computing for the research reported in this paper was done, in part, with equipment purchased with funds provided by an NSF SCREMS grant award DMS 9707740 to the Department of Statistics at Iowa State University.

## References

- Boulanger, M., and Escobar, L. A. (1994), Experimental design for a class of accelerated degradation tests. *Technometrics* **36**, 260-272.
- Box, G. E. P., and Cox, D. R. (1964), An analysis of transformations (with discussion), *Journal of the Royal Statistical Society, Series B* **26**, 211-252.
- Carey M. B., and Koenig, R. H. (1991), Reliability assessment based on accelerated degradation: a case study, *IEEE Transactions on Reliability* **40**, 499-506.
- Carey, M. B., and Tortorella, M. (1988), Analysis of degradation data applied to MOS devices, paper presented at the 6th International Conference on Reliability and Maintainability, Strasbourg, France.
- Dowling, N. E. (1993), *Mechanical Behavior of Materials*, Englewood Cliffs, NJ: Prentice Hall.
- Efron, B. (1985), Bootstrap confidence intervals for a class of parametric problems, *Biometrika* **72**, 45-58.
- Johnston, J. (1972), *Econometric Methods*, New York: McGraw-Hill Book Company.
- Klinger, D. J. (1992), Failure time and rate constant of degradation: an argument for the inverse relationship. *Microelectronics and Reliability* **32**, 987-994.
- Lindstrom, M. J., and Bates, D. M. (1990), Nonlinear mixed effects models for repeated measures data, *Biometrics* **46**, 673-687.
- Lu, C. J., and Meeker, W. Q. (1993), Using degradation measures to estimate a time-to-failure distribution. *Technometrics* **34**, 161-174.
- Meeker, W. Q., and LuValle, M. J. (1995), An accelerated life test model based on reliability kinetics, *Technometrics* **37**, 133-146.
- Murray, W. P. (1993), Archival life expectancy of 3M magneto-optic media, *Journal of the Magnetics Society of Japan* **17**, Supplement S1, 309-314.

- Murray, W. P. (1994), Accelerated service life prediction of compact disks, in *Accelerated and Outdoor Durability Testing of Organic Materials, ASTM STP 1202*, Warren D. Ketola and Douglas Grossman, Editors, Philadelphia: American Society for Testing and Materials.
- Murray, W. P., and Maekawa, K. (1996), Reliability evaluation of 3M magneto-optic media, *Journal of the Magnetics Society of Japan* **20**, Supplement S1, 309-314.
- Nelson, W. (1990), *Accelerated Testing: Statistical Models, Test Plans, and Data Analyses*, New York: John Wiley & Sons, Inc.
- Nelson, W. (1995), Defect initiation and growth—a general statistical model & data analysis. Paper presented at the 2nd annual Spring Research Conference, sponsored by the Institute of Mathematical Statistics and the Physical and Engineering Section of the American Statistical Association, Waterloo, Ontario, Canada, June 1995.
- Palmer, M. J., Phillips, B. F., and Smith, G. T. (1991), Application of nonlinear models with random coefficients to growth data, *Biometrics* **47**, 623-635.
- Pinheiro, J. C., and Bates, D. M. (1995a), Approximations to the loglikelihood function in the nonlinear mixed effects model, *Journal of Computational and Graphical Statistics* **4**, 12-35.
- Pinheiro, J. C., and Bates, D. M. (1995b), Mixed effects models, methods, and classes for S and Splus. Department of Statistics, University of Wisconsin. Available from Statlib.
- Rosenblatt, M. (1952), Remarks on a multivariate transformation, *Annals of Mathematical Statistics* **24**, 470-472.
- Shao, J., and Tu, D. (1995), *The Jackknife and Bootstrap*, New York: Springer.
- Shiomi, H., and Yanagisawa, T. (1979), On distribution parameter during accelerated life test for a carbon film resistor, *Bulletin of the Electrotechnical Laboratory* **43**, 330-345.
- Sobczyk, K. and Spencer, B. F. (1992), *Random Fatigue: From Data to Theory*, San Diego: Academic Press.
- Suzuki, K., Maki, K., and Yokogawa, S. (1993), An analysis of degradation data of a carbon film and properties of the estimators, in *Statistical Sciences and Data Analysis*, (K. Matusita, M. Puri, and T. Hayakawa, Editors), Utrecht Netherlands: VSP.
- Tobias, P. A., and Trindade, D. C. (1995), *Applied Reliability* (Second Edition), New York: Van Nostrand Reinhold Co.
- Tseng, T. S., Hamada, M., and Chiao, C. H. (1995), Using degradation data from a factorial experiment to improve fluorescent lamp reliability, *Journal of Quality Technology*, **27**, 363-369.
- Tseng, S. T., and Yu, H. F. (1997), A termination rule for degradation experiment, *IEEE Transactions on Reliability* **46**, 130-133.